Aspects of Molecular Medicine 2 (2023) 100019

Contents lists available at ScienceDirect

Aspects of Molecular Medicine

journal homepage: www.journals.elsevier.com/aspects-of-molecular-medicine

Morin hydrate promotes nephrin expression through modulation of Notch1-Snail signalling pathway in diabetic rats

Akeem Olalekan Lawal [a], Ibukun Mary Folorunso [a,b,*], Olufemi Adebisi [a], Omowumi Funmilayo Koledoye [a], Opeyemi Iwaloye [a,c]

[a] Bioinformatics and Molecular Biology Unit, Department of Biochemistry, School of Sciences, Federal University of Technology, Akure, P.M.B. 704, Akure, Ondo-State, Nigeria
[b] Precision Molecular Laboratory, Akure, Ondo State, Nigeria
[c] Teady Bioscience Laboratory, Akure, Ondo State, Nigeria

ARTICLE INFO

Handling Editor: Prof A Angelo Azzi

Keywords:
Notch1/snail signalling pathway
Molecular docking
diesel exhaust particles
morin hydrate
Glomerular filtration

ABSTRACT

Reduction in nephrin expression is usually observed in patients with diabetic nephropathy, and there is evidence that Notch1/Snail signalling pathway is essential for the expression of nephrin. This study investigated the role of morin hydrate (MH) on Notch1/Snail signalling pathway in the kidney of type-2 diabetic rats (T2D) exposed to diesel exhaust particles (DEP). The male wistar rats (n = 40) were group into 8 groups: Group 1-Control; Group 2-DEP (0.5 mg/kg); Group 3-type-2 diabetic rat (T2D); Group 4-T2D + DEP (0.5 mg/kg); Group 5-DEP (0.5 mg/kg) + MH (30 mg/kg); Group 6-T2D + MH (30 mg/kg); Group 7-T2D + DEP 0.5 mg/kg + MH 30 mg/kg; and Group 8-MH (30 mg/kg) only. Type-2 diabetes was induced in the rats through a one-time administration of STZ at 45 mg/kg after 14 days treatment with fructose solution at 20% w/v. The type-2 diabetic and non-diabetic rats were exposed to DEP at 0.5 mg/kg through nasal instillation every 48 h for 14 days. MH (30 mg/kg) was given orally every 24 h for 15 days. MH is a naturally occurring flavonoid chemical found in a variety of plants, and has been discovered to have a number of biological actions, including antioxidant, anti-inflammatory, and anticancer effects. The effect of MH on kidney function indices and electrolytes, and its modulatory role on Notch1/Snail signalling pathway were determined. *In silico* studies on binding affinity of MH with some proteins in this pathway was conducted and the electronic behavior of MH was predicted using DFT calculation. The results show that MH oral therapy ameliorates nephrotoxicity and protects the podocytes in T2D rats and T2D rats exposed to DEP. It decreased the serum levels of creatinine, urea and total protein, while also decreasing the levels of renal sodium and potassium ions and bicarbonate. MH increased mRNA expression of nephrin by modulating Notch1/Snail signalling pathway, and these results were supported by the molecular docking studies. This study suggests that MH promote glomerular filtration in T2D exposed to DEP.

1. Introduction

Diesel exhaust particles (DEP), also referred to as PM2.5, are fine and ultrafine particles that constitute approximately 20% of the overall ambient particulate matter (PM). Exposure to DEP may aggravate cardiac ischemia, impair endothelial and fibrinolytic activities, and increase blood thrombogenicity (Costello et al., 2018). The metabolic syndrome, which also includes obesity, arterial hypertension, elevated triglycerides (TG) and cholesterol, and alteration of glucose homeostasis, is linked to air pollution and PM (Landrigan et al., 2018; Bowe et al., 2018). Due to its ability to disperse to other tissues, inhaled PM2.5 has been associated with insulin resistance, diabetes and adipose tissue inflammation in rats (Chilian-Herrera et al., 2021; Lawal et al., 2022). However, people living with diabetes or/and hypertension are prone to these effects compared to healthy ones.

Type 2 diabetes (T2D) is a type of diabetes that causes high blood sugar, insulin resistance, and a relative lack of insulin (Pasquel and Umpierrez, 2014). When diabetes is untreated, it results to a number of

* Corresponding author. Bioinformatics and Molecular Biology Unit, Department of Biochemistry, School of Sciences, Federal University of Technology, Akure, P.M.B. 704, Akure, Ondo-State, Nigeria.
E-mail addresses: lawalao@futa.edu.ng (A.O. Lawal), folorunsoim@futa.edu.ng (I.M. Folorunso), adebisiolufemi4@gmail.com (O. Adebisi), omkoledoye@futa.edu.ng (O.F. Koledoye), iwaloyeo@futa.edu.ng (O. Iwaloye).

https://doi.org/10.1016/j.amolm.2023.100019
Received 12 December 2022; Received in revised form 16 June 2023; Accepted 4 July 2023

complications, and among them is diabetic nephropathy. Diabetic nephropathy is most common causes of end-stage renal disease and chronic kidney disease (CKD) worldwide, and it is characterized by persistent decrease of kidney function (Kittell, 2012). Many kinds of CKD have the triad of protein leakage into the urine (proteinuria or albuminuria), increasing blood pressure with hypertension, and finally declining renal function (Afkarian et al., 2016). Massive protein loss in the urine as a consequence of glomeruli destruction may cause widespread body swelling (edema), which is known as nephrotic syndrome. The progression of diabetic nephropathy may be monitored using serum creatinine, a blood test used to determine the estimated glomerular filtration rate (eGFR), which measures the fraction of glomeruli no longer filtering blood, and proteinuria, a marker of how much damage has been done to the glomeruli (Zhu and Zheng, 2021).

The malfunctioning of podocytes, a type of glomerular epithelial cell, is believed to play a significant role in progressive renal disorders, such as diabetic nephropathy (Ma et al., 2013; Yao et al., 2015). Podocyte damage is also connected with an increase in albuminuria. The Notch1/Snail signalling pathway has been identified as playing a pathogenic role in diabetic nephropathy through the promotion of podocyte dysfunction and the loss of glomerular filtration barrier integrity, ultimately leading to proteinuria. Diabetic nephropathy's characteristic functional connection between Notch1 activation and nephrin down-regulation in podocytes is essential to this process. Included among the target RNAs generated by the active Notch1 intracellular domain is Snail, a transcription factor implicated in mesenchymal transition that inhibits nephrin production (Shi et al., 2018). The Notch1/Snail pathway has been identified as the molecular mechanism behind the angiotensin II-induced down-regulation of nephrin in podocytes and the persistence of glomerular damage in patients with diabetic nephropathy (Gagliardini et al., 2013a). In angiotensin II-stimulated podocytes, activation of Notch1 canonical signalling via Hes1 increased the production of Snail and its translocation into the nucleus, resulting in the down-regulation of nephrin. Hence it has been suggested that targeting the Notch1/Snail signalling pathway protects podocytes in diabetic nephropathy (Warren et al., 2019).

Morin hydrate (MH), a natural yellow crystalline polyphenolic compound derived from plant source (Singh et al., 2018), has been shown to exhibit diversity of pharmacological activities, including anti-inflammatory effects, antioxidant and scavenging free radical properties (Lawal et al., 2022). It has been used in the treatment of diseases including diabetes and nephrotoxicity (Paoli et al., 2013). Previous works have also reported the nephroprotective properties of MH (Singh et al., 2018).

In our previous study, we established that MH ameliorates oxidative and inflammatory effects of DEP in pancreas of T2D rats (Lawal et al., 2022). This current study hypothesizes that MH protects the kidney through the inhibition of Notch1/Snail signalling pathway, resulting in increased nephrin expression.

2. Materials and methods

2.1. DEP collection, extract preparation and characterization

The DEP used in this work was collected as previously described (Lawal et al., 2022). The methanol DEP extract was prepared as reported by (Lawal et al., 2015) and has been well characterized in our previous study (Lawal et al., 2022).

2.2. Animal treatment and samples preparation

2.2.1. Diabetes induction

The T2D was induced in rats as previously reported (Lawal et al., 2022). After two weeks of oral fructose treatment at 20% w/v, the rats were administered 45 mg/kg body weight of freshly produced streptozotocin (STZ) in citrate buffered solution (0.1 M, pH 4.5) intraperitoneally. After 72 h of STZ injection, diabetes was confirmed using an ACCU-CHEK compact plus glucometer to assess the fasting blood glucose level. Rats with a glucose level of 200 mg/dl or above were diagnosed with diabetes).

2.2.2. Exposure protocol and tissues harvest

Forty (40) male Wistar rats weighing an average of 95.0 g were purchased from the Biochemistry Department of the Federal University of Technology, Akure (FUTA) and kept in the department's animal facility. These experimental rats were handled in accordance with the FUTA School of Science Animal Ethics Committee. The animals were divided into eight groups of five animals per group (n = 5), The groupings include: Control; DEP (0.5 mg/kg); type-2 diabetic rat (T2D); T2D + DEP (0.5 mg/kg); DEP (0.5 mg/kg) + MH (30 mg/kg); T2D + MH (30 mg/kg); T2D + DEP 0.5 mg/kg + MH 30 mg/kg and MH (30 mg/kg). MH was administered through oral gavage at 30 mg/kg every 24 h for 15 days (Kapoor and Kakkar, 2012). DEP was administered, according to previous study (Yokota et al., 2010), through nasal instillation at 0.5 mg/kg every 48 h for 14 days. The control group had unrestricted access to food and water ad libitum. The DEP rats were exposed to DEP (0.5 mg/kg) through nasal instillation every 48 h for 14 days. T2D was induced in the type-2 diabetic rat (T2D) group. DEP was nasally administered at 0.5 mg/kg every 48 h for 14 days after induction of T2D in the T2D + DEP (0.5 mg/kg) group. In DEP (0.5 mg/kg) + MH (30 mg/kg), after exposure to DEP at 0.5 mg/kg, the experimental rats were orally treated with MH at 30 mg/kg every 24 h for 15 days. The T2D + MH (30 mg/kg) group was treated with MH at 30 mg/kg every 24 h for 15 days. In T2D + DEP 0.5 mg/kg + MH 30 mg/kg group, the T2D rats were exposed to DEP at 0.5 mg/kg every 48 h for 14 days after which they were treated with MH at 30 mg/kg every 24 h for 15 days through oral gavage. MH was orally administered at 30 mg/kg every 24 h for 15 days in the MH (30 mg/kg) group. Twenty-four (24) hours following the final treatment, all animals were slaughtered. The kidney was removed and stored at −80 °C for subsequent assays.

2.3. Processing of blood samples and tissue homogenate

Blood was drawn into a new test vial and left to clot at room temperature for 30 min. Ten minutes of centrifugation at 2000 rpm separated the serum. About Two hundred and 50 mg (250 mg) of kidney tissues were chopped into fragments and homogenized in a saline solution to provide 20% homogenate (w/v). The homogenate was centrifuged at 1000 rpm for 10 min. The supernatant was separated and utilized for many subsequent biochemical analyses.

2.4. Determination of biochemical parameters

The levels of serum and kidney creatinine, urea and total protein were determined using the commercially available Randox kits.

2.5. RNA isolation and quantification

The kidney tissue was homogenized in Trizol reagent obtained from Inqaba Biotech, Africa Genomics Company (South Africa). The homogenate was treated with a gradient separation media (chloroform) and centrifuged for 30 min at 1500 rpm. The supernatant was added to 100 μL of precipitating medium (isoamyl alcohol) and vortexed at 1500 rpm for 30 min to recover the RNA pellet. The supernatant was then decanted. The precipitated RNA was suspended in water devoid of nucleases. To eliminate any DNA and phenol contamination, DNase digestion and subsequent re-precipitation in ethanol were done. The total RNA concentration was then measured by UV absorbance spectrophotometry (JENWAY 6305).

2.6. Complementary deoxyribonucleic acid (cDNA) synthesis and polymerase chain reaction (PCR)

Total RNA was reverse-transcribed into cDNA by reverse transcription reaction (RT) using Protoscript II reverse transcription kit (Inqaba Biotech, South Africa). The synthesized cDNA was diluted in Nuclease-free water and 5 μL was aliquoted into a PCR cocktail. The PCR reaction mix contains 5 μL cDNA template, 2 μL forward and reverse primers, and 4 μL PCR Master Mix. The PCR amplification was done under 35 cycles using appropriate primers (Table 1) and β-actin was used as a housekeeping gene to normalize the expression of the target genes.

2.7. Agarose gel electrophoresis

The amplified genes were separated by electrophoresis on 0.8% agarose gels in 1*X* Tris-base glacial acetic acid-EDTA-TAE buffer (pH 7.0), and the bands were quantified using image j software. To normalize the relative expression levels of the other genes, the gene β-actin was used. Under UV-gel documentation, pictures showing the relative density of DNA bands were obtained. Using Image J software (http://imagej.en.softonic.com/), the band intensities were densitometrically measured.

2.8. In silico study

2.8.1. Protein retrieval and preparation

The protein crystal structure of nephrin, angiotensin II and noctch1 with PDB ID of 4 ZR T, 5UNF and 2VJ3 were downloaded from protein databank. The proteins were exported to maestro graphical interface, and prepared to remove the water molecules, optimized the hydrogen bonds and minimized the structure using OPLS3 force field.

2.8.2. Receptor grid generation

The receptor grid files were generated picking the ligand binding to the proteins. This allows the compound of interest to interact with the protein within its binding pockets. The X, Y and Z coordinates supplied for Notch1 are −20.41, 9.24 and −22.56; the coordinates supplied for Nephrin are 18.96, −5.75 and −7.53, respectively. Finally, the supplied X, Y and Z, coordinates for angiotensin II are 64.81, 12.15 and 5.68.

2.8.3. Optimization of MH chemical structure

The 2D structure of MH was downloaded from Pubchem database (https://pubchem.ncbi.nlm.nih.gov/) and uploaded into the workspace of Maestro material science. The compounds were optimized density functional theory (DFT) with B3LYP-D3 as level of theory and 6-31G** as the basis set. The convergence criteria were left as default and the maximum steps for the optimization was tuned to 100.

2.8.4. Molecular docking

The compound MH was docked with the proteins using glide extra precision (XP) docking to reveal the binding affinities of the compounds with the respective proteins.

Table 1
Primers for polymerase chain reaction.

Genes Sequence
β actin Forward: CTCCCTGGAGAAGAGCTCATGA
Reverse: AGGAAGGAAGGCTGGAAGA
KIM-1 Forward: ACCGACTAAGGGCTTCTAT
Reverse: CAGGAGCTGGAATGGGTATTT
Angiotensin II Forward: GTTGGAACGCTGCCATTTAC
Reverse: AAAGTGGTGGGAGATGAAGC
NOTCH 1 Forward: CAGGAGGATGCAGGCAATAA
Reverse: ATTGAAGTTGAGGGGAGCAGTC
SNAIL 1 Forward: TTTGCTGCAGATGGCTGAT
Reverse: ACCTAAAGCCAACCCACTGG
NEPHRIN Forward: TGAAGCTGGACGTGCATTAT
Reverse: GTCAACGGTGCAGACTATGT

2.8.5. Binding free energy calculation

The protein-ligand complex was incorporated to the module panel of MM-GBSA to determine the stability of the complex.

2.8.6. Calculation of the electronic behavior of MH

Using B3LYP-D3 level of theory and 6-31G** basis set at theory settings for DFT, the electronic behavior of MH was calculated. This study adopted polarizable continuum model (PCM), a solvent model that uses a molecule-shaped cavity and the full molecular electrostatic potential to obtain apparent surface charge. DMSO was selected as the solvent because, during the wet experiment, the compound was dissolved in DMSO prior to being administered to the diabetic rats.

2.9. Statistical analysis

GraphPad 5 Software was used to analyze the data using one-way analysis of variance (ANOVA) (USA). The results were presented as mean ± SD. We made numerous comparisons between the two groups using the Bonferroni post-hoc test. When the p-value was less than 0.05, the differences were determined to be statistically significant.

3. Results

3.1. MH lowers the fasting blood glucose level in T2D rats exposed to DEP

The T2D was confirmed in the rats at the fourth week after treatment as reported in our previous study (Lawal et al., 2022). However, further exposure of these diabetic rats to 0.5 mg/kg DEP did not cause any significant alteration on the fasting blood glucose levels for up to 9 weeks (Fig. 1). Treatment of the diabetic rats with 30 mg/kg MH caused significant ($p < 0.05$) reduction in the fasting blood glucose level. Similarly, post-treatment of T2D rats that were exposed to DEP (T2D-DEP) with MH (MH) caused significant ($p < 0.05$) decrease in fasting blood glucose level below 200 mg/dl from week 8 to week 9, indicating its anti-diabetic effect even in the presence of DEP (Fig. 1).

3.2. MH ameliorates the serum levels of renal dysfunction indices induced in T2D rats exposed to DEP

The results in Fig. 2 show the effects of MH on serum level of creatinine (Fig. 2 A), urea (Fig. 2 B) and total protein (Fig. 2C) in T2D rats exposed to DEP. There were elevated levels of creatinine, urea and total protein which signify renal damage in diabetic rats and diabetic rats exposed to DEP. These effects were however, reversed in MH treatment groups. For serum creatinine level (Fig. 2 A), there was a significant ($p < 0.05$) increased in creatinine level in the T2D and T2D-DEP 0.5 groups when compared to the control group, and significant ($p < 0.05$) decreased in creatinine level upon administration of MH to the rats, when compared to diabetic control and diabetic rats exposed to DEP. The result also shows that urea level was significantly ($p < 0.05$) increased in diabetic rats and diabetic rats exposed to DEP when compared to normal rats and significantly ($p < 0.05$) decreased in groups treated with MH when compared with T2D and T2D-DEP 0.5 (Fig. 2 B). Serum total protein level (Fig. 2 C) was significantly ($p < 0.05$) increased in T2D and DEP exposed rats when compared to normal rats but significantly ($p < 0.05$) decreased in MH treatment groups when compared to T2D and T2D-DEP 0.5 (see Fig. 3).

3.3. MH reduces the elevated kidney electrolytes levels in T2D rats exposed to DEP

The results in Fig. 4 A, B and C show that MH significantly ($p < 0.05$) increased the levels of sodium, potassium and bicarbonate ions in T2D rats and T2D rats exposed to DEP (T2D-DEP 0.5). However, MH significantly ($p < 0.05$) lowered the sodium (Fig. 4 A), potassium (Fig. 4 B) and bicarbonate (Fig. 4C) ions level in the kidney of the T2D. Also, MH

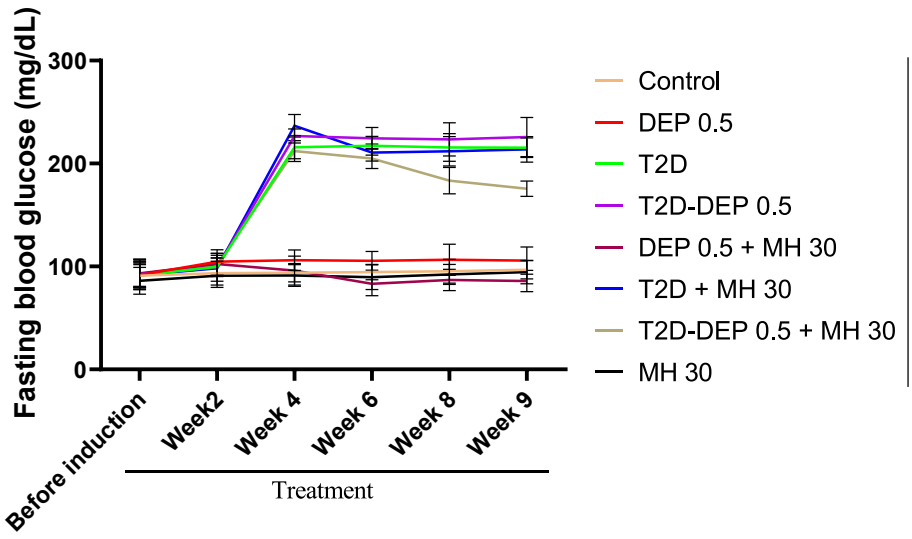

Fig. 1. The fasting blood sugar (FBS) of the experimental rats.

significantly ($p < 0.05$) lowered the levels of sodium (Fig. 4A), potassium (Fig. 4B) in T2D exposed to DEP but there was no significant difference in the level of bicarbonate in T2D rats exposed to DEP treated with MH compared to T2D rats exposed DEP.

3.4. MH activates nephrinogenesis via angiotensin II/Notch1/snail pathway in the kidney of T2D rats exposed to DEP

The results in Fig. 5 show that there were significant ($p < 0.05$) increased in the gene expressions of angiotensin II (Fig. 5 A), notch 1 (Fig. 5 B) and snail (Fig. 5C) in the groups of DEP (0.5 mg/kg), T2D, and T2D-DEP (0.5 mg/kg) compared to control. In contrast, nephrin mRNA level was significantly ($p < 0.05$) decreased in the groups of DEP (0.5 mg/kg), T2D, and T2D-DEP (0.5 mg/kg) compared to control (Fig. 5 D). Posttreatment with MH caused a significant ($p < 0.05$) reversal in the expressions of these genes. The flavonoid caused significant decreased in the mRNA levels of angiotensin II, Notch1 and snail, while at the same time significantly increased nephrin mRNA level when compared to DEP (0.5 mg/kg) and T2D-DEP (0.5 mg/kg) groups (Fig. 5).

3.5. MH mitigates KIM1 gene expressions induced in the kidney of T2D rats exposed to DEP

The result in Fig. 6 shows that there was significant ($p < 0.05$) increased in the expression of KIM1 in the DEP (0.5 mg/kg), T2D, and T2D-DEP (0.5 mg/kg) rats compared to control. There was significant ($p < 0.05$) decreased in the expression in MH treated groups of T2D and T2D-DEP (0.5 mg/kg) compared to T2D group. Also, the result shows a significant ($p < 0.05$) increase in DEP (0.5 mg/kg) group treated with MH (30 mg/kg) compared to DEP (0.5 mg/kg) group.

3.6. In silico study of MH with molecules of Notch1/Snail signalling pathway

The molecular docking results are provided in Tables 2 and 3 and 4. MH had docking scores of −6.981 kcal/mol with angiotensin II (Table 2). MH interacts to form non-covalent interactions including H-bond and pi-pi interactions with Lys215 and Thr178 amino acid residues. On the other hand, metformin interacted with Tyr51 and Tyr108. The 2D and 3D interaction plots are given in Fig. 7. Furthermore, the binding free energy (ΔG Bind) result shows that the complexes are stable, which depicts the reliability of the docking scores obtained by the ligand bound protein. MH-angiotensin II complex had ΔG Bind score of −30.88 kcal/mol.

In Table 3, the docking score and post docking analysis are provided. Again, MH had the high docking score upon binding to the catalytic domain of nephrin. MH had docking scores of −5.576 kcal/mol (Table 3). It formed interactions with hydrophobic amino acid residues, as evidence in Fig. 8. Specifically, MH formed salt bridge, H-bond and pi-pi interactions with Lys120, Arg221, Tyr46 residues. These interactions may be responsible for the moderated binding affinity attained by the compound upon binding to the binding pockets of nephrin. The binding free energy results provided by MM-GBSA module demonstrated the stability of the complex; MH had a binding free energy score of −24.82 kcal/mol with nephrin (Table 3). The docking score of MH with Notch1 is given in Table S3. It has a docking score of −6.801 kcal/mol, and formed H-bond network with Asn454, Asn459, Ala465 residues, and these residues occupy the binding pocket of Notch1 (Fig. 9). In brief, the two compounds formed stable complexes with Notch1. It is also shown from the results that Coulomb energy, van der Waals energy, hydrogen bond are the major contributors to MH 'binding free energy (Tables 2–4).

3.7. Electronic behavior of MH in DMSO

The results of the electronic behavior of MH are given in Fig. 10. The frontier molecular orbitals (FMOs) are used to describe the molecular properties of low-molecular weight organic compound, and they include the highest occupied molecular orbital (HOMO) and the lowest unoccupied molecular orbital (LUMO). The LUMO term refers to the electron-accepting region of a compound, on the other hand, the HOMO term investigates the compound's electron-donating site (Olawale et al., 2022). The energy band gap, which is determined by contrasting the HOMO and LUMO states of a compound, is useful for determining both the chemical reactivity and the stability of a molecule (Olawale et al., 2022a). According to the estimated electronic behavior MH in liquid (DMSO) phase following computing using DFT calculation, MH had HOMO value of −0.19180 eV and LUMO value of −0.04616 eV (Fig. 10 A and B), with energy gap is 0.14564 eV. Previous study has shown that molecule with low energy gap has high reactivity, and based on this hypothesis, we confer that MH is reactive when dissolve in DMSO, and this may provide some of the basis for its therapeutic efficacy in the treatment of diabetes.

Consequently, the compound's molecular electrostatic potential (MESP) was determined to understand how charges are distributed across the atomic sites of MH (Fig. 10C). This allowed for the identification of the sites within the compound that were most electropositive (and therefore vulnerable to nucleophilic attack) and electronegative

A

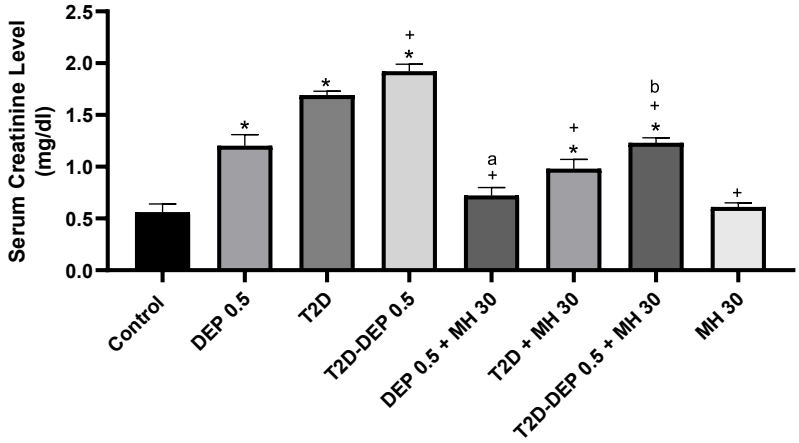

B

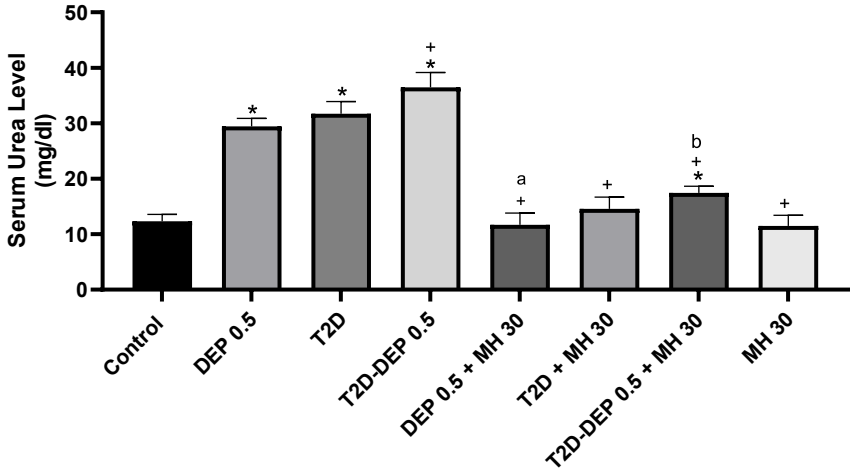

C

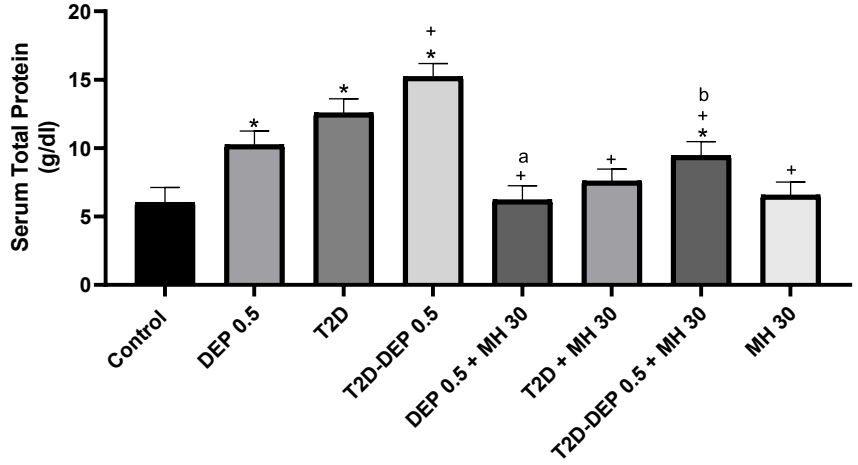

Fig. 2. Effects of MH on serum renal dysfunction indices in type-2-diabetic rats exposed to DEP. Type-2-diabetic rats were exposed to DEP prior to MH treatment. (A) Creatinine (B) urea (C) total protein levels were determined in the serum as described in the materials and methods.

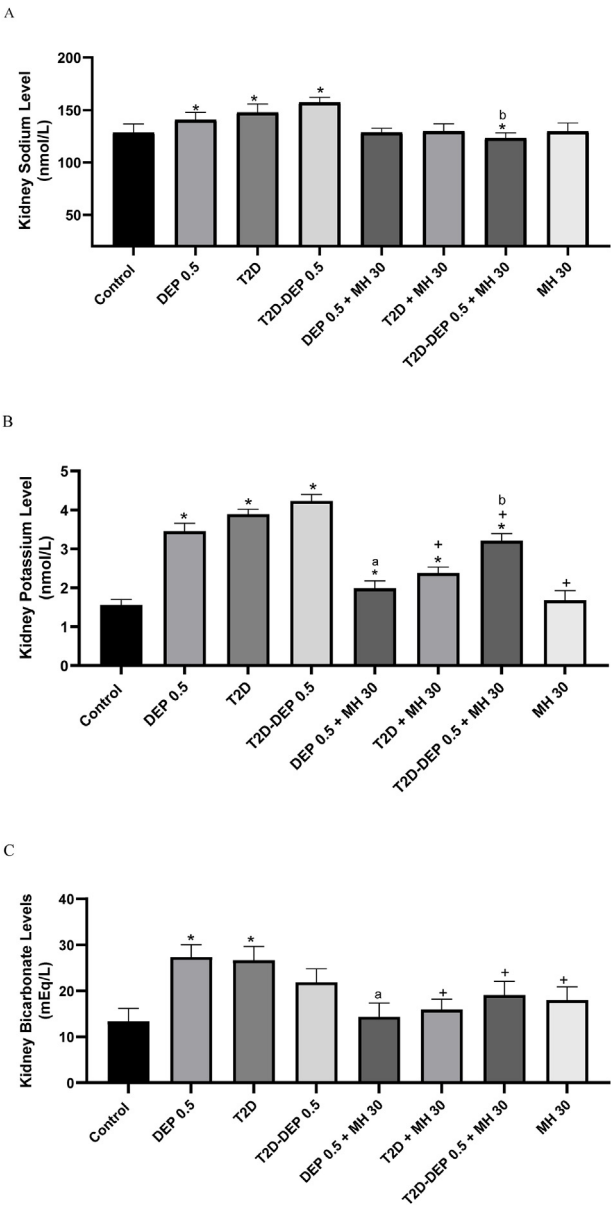

Fig. 3. Effects of MH on kidney electrolytes levels in type-2-diabetic rats exposed to DEP. Type-2-diabetic rats were exposed to DEP prior to MH treatment. (A) Sodium, (B) potassium and (C) bicarbonate ions levels were determined in the kidney as described in the materials and methods.

(and thus vulnerable to electrophilic attack). The electronegative atomic site of MH is found at the oxygen atom attached to carbon atom at position 14. However, the regions prone to nucleophilic attack are distributed across the compound. These sites may give information on the atoms of compounds capable of forming non-covalent bonds (Elekofehinti et al., 2021).

The Fukui function notion is beneficial for acquiring a greater understanding of the density-dependent reaction or reactivity features of chemicals (Elekofehinti et al., 2021). This means that using Fukui parameters, the atomic sites of a chemical compound that are vulnerable to nucleophilic and electrophilic attack may be easily detected. There are two functions: one for increasing the number of electrons (f+) and one for decreasing the number of electrons (f-). In Fig. 10 D and E, the f+ and f-of MH were following fukui function calculation, with blue region and red regions depicting positive and negative charge, respectively. The regions of positive charges in Fig. 10 D (f+) are sites where there was an increase in electron density following addition of charges whereas location of negative charges in Fig. 10 E (f-) are atomic sites with decreased in electron density after removal of charge.

4. Discussion

This work examined the effect of MH on DEP toxicity in T2D wistar rats and it confirmed that MH improve the renal function of T2D wistar rats exposed to DEP by reducing the serum levels of urea, creatinine and total protein; increasing the sodium, potassium and bicarbonate ions levels in the kidney. Also, this study established that MH modulates Notch1/Snail signalling pathway to preserve glomerular filtration and podocytes.

The DEP have been linked to a number of human diseases, including cardiovascular, neurological, and urinary system disorders (Sylla et al., 2017; Yaser et al., 2014), due to its ability to disperse to other tissues, where they may cause inflammatory reactions, disruption in the control of vascular tone, and fibrinolysis (Albano et al., 2022). These effects are particularly noticeable in those who have diabetes or hypertension (Tong et al., 2012). However, only about 20–40 percent people with diabetes develop nephropathy, suggesting that particular genetic and/or environmental variables have a role in the onset and course of the disease (Tonneijck et al., 2017; Gheith et al., 2016).

The glomerular filtration rate (GFR), commonly known as the glomerular filtration capacity is determined by measuring creatinine concentrations in serum and urine samples (Mora-Fernández et al., 2014). The glomerulus filters creatinine that is generated intracellularly inside the body. Creatinine is a valuable endogenous biomarker for creatinine clearance because of these properties (Salazar, 2014). When the GFR declines, as it does in renal impairment, the renal system's ability to remove creatinine is reduced. As a result of the lower GFR, the serum creatinine concentration would rise (Ciobanu et al., 2013). However, renal function cannot be assessed only on the basis of serum creatinine because the levels of creatinine in the blood may not be impacted until the kidneys have been severely damaged (Kittell, 2012). Here, we report significant increase in the serum creatinine levels of T2D rats exposed to DEP. This creatinine clearance effect of MH is in accordance with previous work of (Griffin et al., 2019; Aleisa et al., 2013). As an indicator of renal function, a high-protein diet, protein synthesis variables, and patient hydration status may all affect urea levels, making it less specific than creatinine. When used alone, urea isn't the greatest indicator of glomerular filtration rate (GFR) but in combination with plasma creatinine, the creatinine/BUN ratio may assist differentiate between increases in serum that occur before and after renal treatment. The increase in serum urea level in T2D as seen in this study has been reported in previous work (Liu et al., 2022; Dal Canto et al., 2019). Exposure of these T2D rats to DEP significantly elevate the serum levels of urea and treatment with MH was able to significantly reverse these effects. This reducing effect of MH on serum urea level in nephrotoxicity is in agreement with previous studies (Adachi et al., 2020).

Persistent proteinuria has been reported as a symptom of overt diabetic nephropathy. Proteinuria is preceded by phases of excessive glomerular filtration and microalbuminuria in the natural course of T2D, indicating an elevated potential of development to overt nephropathy (Zhu and Zheng, 2021). Renal failure may be detected by an increase in proteinuria, which is a sign of decreasing renal function (Zhu and Zheng, 2021). Proteinuria is caused by glomerular damage and increased macromolecule permeability in the glomerulus and may be used to determine the severity of diabetic glomerulopathy (Ciobanu et al., 2013). Heavy proteinuria is closely linked to pathological alterations in the diffuse and, less typically, the nodular forms of diabetic glomerulosclerosis in diabetic nephropathy (Zhu and Zheng, 2021). For every postulate of the proteinuria hypothesis, determining the mechanisms of proteinuria particular to diabetes is critical (Pálsson and Patel, 2014). Enhanced glomerular filtration, insufficient tubular absorption, overflow, and increased tubular secretion are the four processes identified for excessive protein excretion in general; however glomerular filtration is

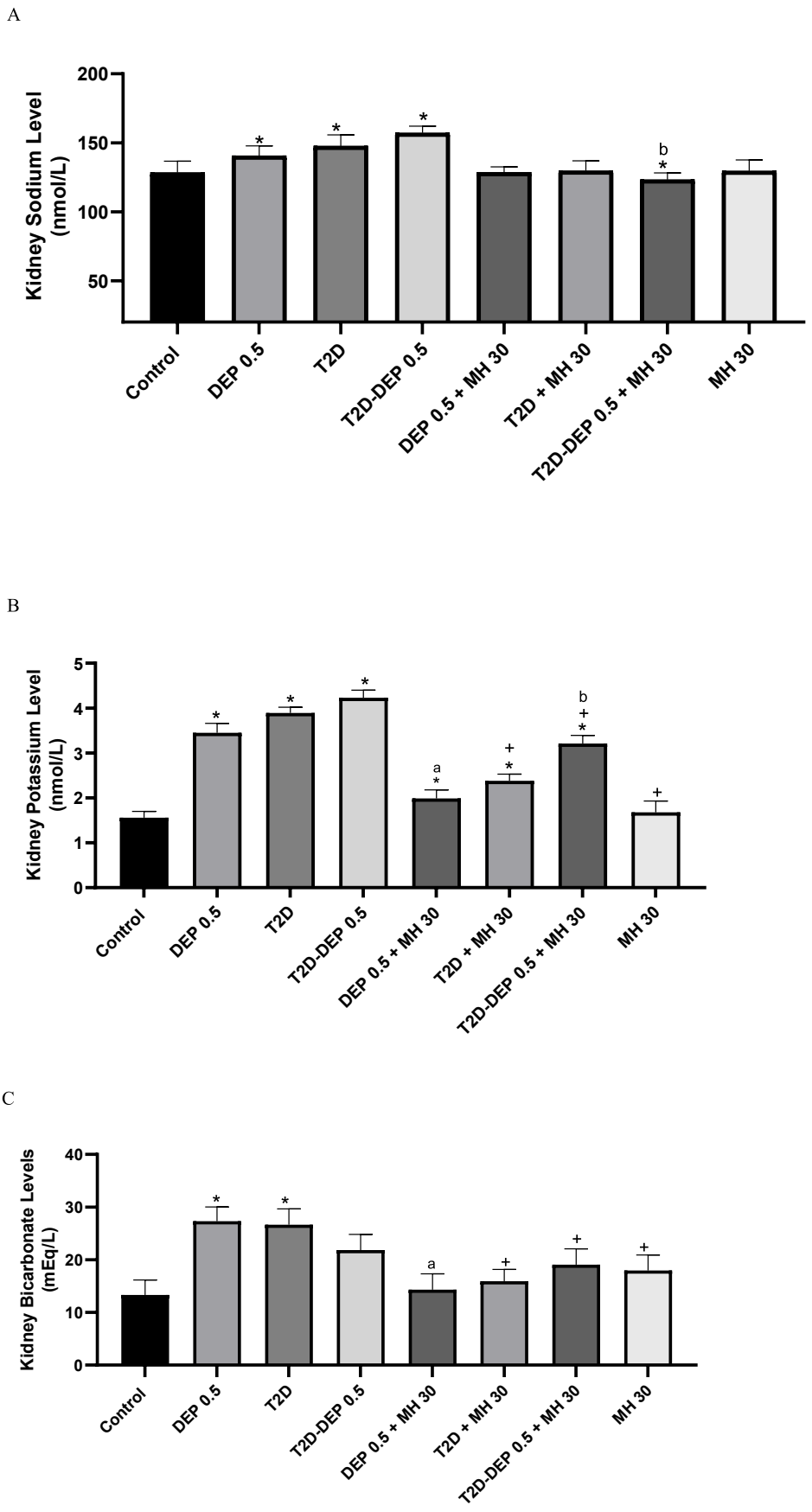

Fig. 4. Effects of MH on angiotensin II/notch 1/snail/nephrin pathway in type-2-diabetic rats exposed to DEP. Type-2-diabetic rats were exposed to DEP prior to MH treatment. The mRNA levels of (A) Angiotensin II, (B) Notch 1, (C) Snail and (D) Nephrin were quantified by RT-PCR.

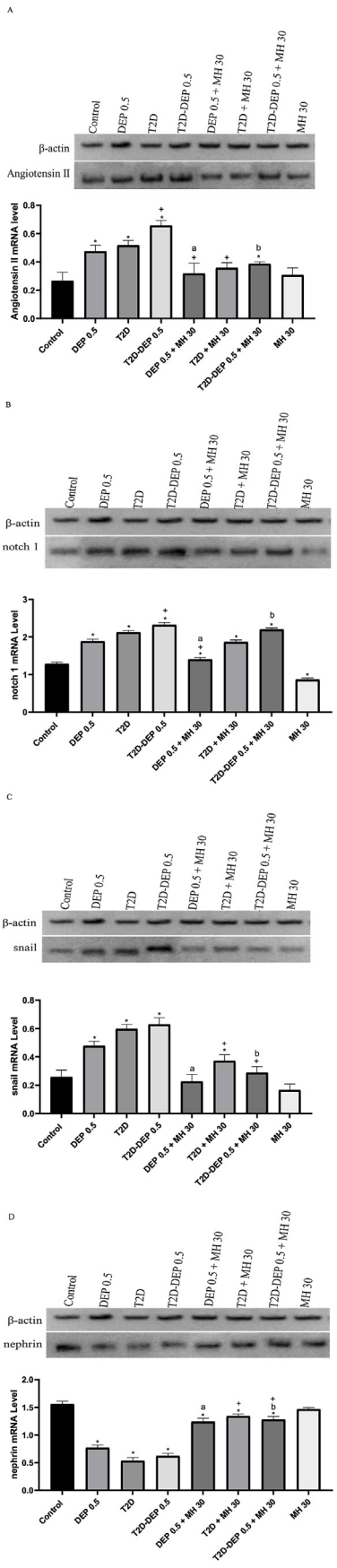

Fig. 5. Effects of MH on KIM 1 gene expression in type-2-diabetic rats exposed to DEP. Type-2-diabetic rats were exposed to DEP prior to MH treatment. The mRNA levels of KIM 1 were quantified by RT-PCR.

the most prevalent (Afkarian et al., 2016). This study demonstrated a significant increase in the serum total protein level in T2D rats and T2D rats exposed to DEP which is in support of previous works (Ciobanu et al., 2013; Moosaie et al., 2021). However, treatment with MH significantly decrease the serum total protein level due to the compound's glucose lowering properties, which has been reported in previous studies (Aleisa et al., 2013; Rajput et al., 2021).

Renal ion transporters play a crucial role in the pathophysiology of diabetic kidney disease and its development. Ion transport in the kidney may be affected by hyperglycemia in a number of ways. As the condition progresses, the glomerular filtration rate (GFR) decreases by more than 50%, causing proteinuria which is a main contributor of renal injury including interstitial fibrosis and glomerulosclerosis (Vallon and Komers, 2011). At earlier stage of diabetic kidney disease, GFR is not significantly reduced. However, as DKD advances, GFR declines following hyperfiltration. The initial hyperfiltration is as a result of the kidneys' effort to compensate for hyperglycemia's decreased salt supply. Kidney function and GFR decline when the tubuloglomerular feedback system's capacity to adjust for increased salt and glucose reabsorption is saturated (Vallon and Komers, 2011; Tuttle, 2017). Klemens et al. has reported that increased Na + retention has been related to the development of hypertension associated with obesity and metabolic diseases particularly diabetes (Klemens et al., 2019). Glycosuria, a key and diagnosable characteristic of diabetes, causes dehydration by glucose osmotic diuresis. Dehydration is accompanied by a significant loss of electrolytes such as sodium, potassium, calcium, chloride, and phosphates (Gaw et al., 1995). Ketone body production is also abnormally enhanced in diabetes, resulting in ketonuria. Ketone bodies, being moderately strong acids, excrete buffer cations, notably alkaline cations (Na+ and K+), as well as bicarbonates (Ramsey et al., 1986). Serum sodium, potassium and bicarbonate levels were observed in this study to be significantly increased in T2D rats exposed to DEP and significantly reduced in DEP exposed T2D rats exposed to DEP.

Podocytes are highly specialized epithelial cells that constitute the visceral epithelial cells of renal glomeruli. The slit diaphragm, which is a unique cell–cell connection between adjacent podocytes in a normal kidney, prevents loss of plasma protein during ultrafiltration (Raines et al., 2022). Studies have found that podocyte injury causes tubular damage and interstitial fibrosis, as well as proteinuria, by disrupting the slit diaphragm, and severe podocyte injury is the first step leading to glomerular sclerosis, which is the final stage of glomerular injury (Maremonti et al., 2022). Many molecules, including nephrin, neph1, and members of the cadherin superfamily, make up the slit diaphragm (Li and Siragy, 2014). Nephrin, a member of the immunoglobulin superfamily, is one of the most important components of these molecules (Welsh and Saleem, 2012). Mice lacking nephrin has been reported to show signs of podocyte damage, including severe proteinuria and effacement of podocyte foot processes (Raines et al., 2022; Jeong et al., 2015; Chen et al., 2021). Slit diaphragm proteins nephrin and podocin are produced by podocytes and they are required for the glomerular basement membrane's sieving functions to be maintained (Gagliardini et al., 2013a).

Angiotensin II infusion into the renal artery of the rat kidney resulted in nephrin loss and effacement of podocyte foot processes, as well as an increase in proteinuria (Gagliardini et al., 2013a). Angiotensin II synthesis blockers protect nephrin inside the slit diaphragm in diabetic rats (Gagliardini et al., 2013b). Angiotensin II decreases nephrin through a transmembrane receptor identified as Notch1. Notch1 is involved in the differentiation of cells and the development of the kidneys. When the Notch1 receptor is engaged, the active Notch1 intracellular domain (ICN1) is released and translocated to the nucleus. Upon activation, otch1 stimulates the snail transcription factor, which is found in the cytoplasm of podocytes. Both ICN1 and snail translocate to the nucleus in response to Angiotensin II signalling, where they contribute to the inhibition of nephrin production, activation of apoptosis and podocyte loss (Gagliardini et al., 2013a). There are strong evidences that the Notch1 pathway is a prevalent mechanism of podocyte damage through down-regulation in

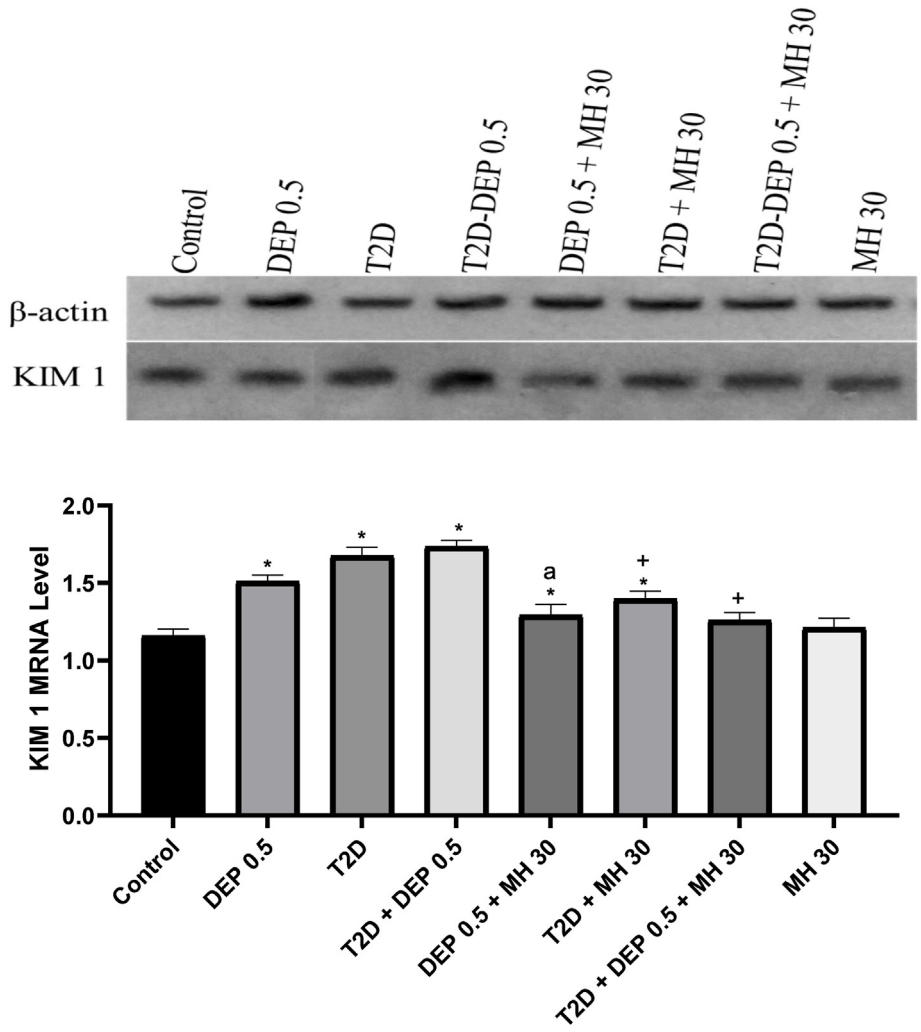

Fig. 6. Two- and three-dimensional interaction diagram between MH and Angiotensin converting enzyme 2.

Table 2
Docking and post-docking analysis of morin hydrate and metformin with Angiotensin II.

Compound name	Molecular docking studies				Binding free energy			
	Docking score	Interacting residues	No of H-bond	No of pi-pi interaction	ΔG_{Bind}[a]	ΔG_{Bind}[b] H-bond	ΔG_{Bind}[c] Coulomb	ΔG_{Bind}[d] vdW
Morin hydrate	−6.981	Lys215, Thr178	2	2	−30.88	−1.80	−17.78	−38.97

[a] MM-GBSA free energy (kcal/mol) of binding.
[b] Contribution to the MM-GBSA free energy of binding (kcal/mol) from hydrogen bond.
[c] Contribution to the MMGBSA free energy of binding (kcal/mol) from the van der Waals energy.
[d] Contribution to the MM-GBSA free energy of binding (kcal/mol) from the Coulomb energy.

Table 3
Docking and post-docking analysis of morin hydrate and metformin with nephrin.

Compound name	Molecular docking studies				Binding free energy			
	Docking score	Interacting residues	No of H-bond	No of pi-pi interaction	ΔG_{Bind}[a]	ΔG_{Bind}[b] H-bond	ΔG_{Bind}[c] Coulomb	ΔG_{Bind}[d] vdW
Morin hydrate	−5.576	Lys120, Arg221, Tyr46	1	1	−24.82	−1.80	−122.33	−27.41

[a] MM-GBSA free energy (kcal/mol) of binding.
[b] Contribution to the MM-GBSA free energy of binding (kcal/mol) from hydrogen bond.
[c] Contribution to the MMGBSA free energy of binding (kcal/mol) from the van der Waals energy.
[d] Contribution to the MM-GBSA free energy of binding (kcal/mol) from the Coulomb energy.

the renal mRNA expression of nephrin (Maremonti et al., 2022). Gagliardini et al. also show that in diabetic nephropathy (DN), Notch1 and snail signalling are consistently active in podocytes, which is a primary molecular mechanism for reduced nephrin expression. As a result, increasing snail podocyte expression may lower nephrin expression, resulting in podocyte damage in DN (Gagliardini et al., 2013a). In

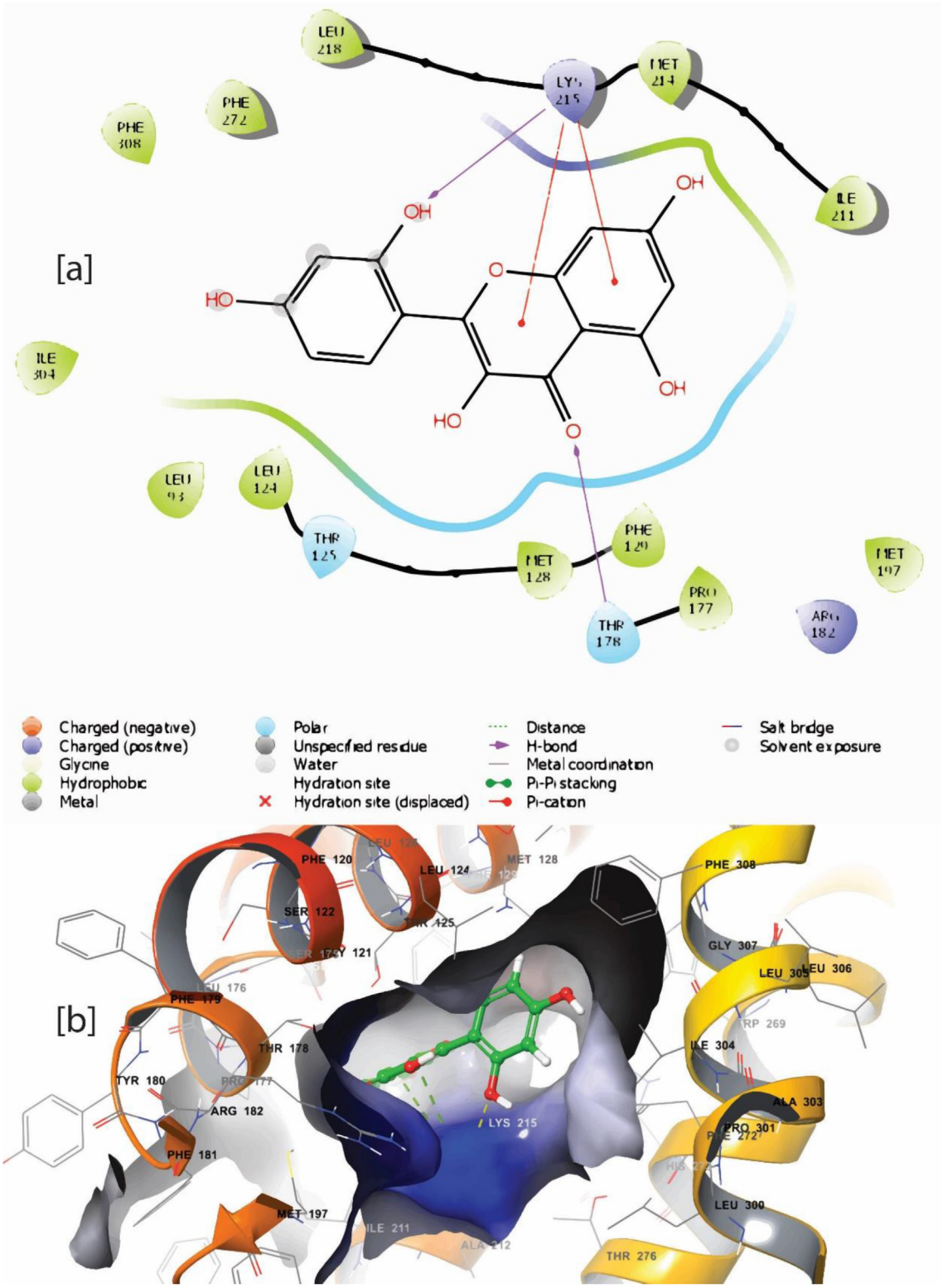

Fig. 7. Two- and three-dimensional interaction diagram between MH and nephrin.

accordance with these previous reports, this study showed a significant increase in the expression of Angiotensin II, Notch1 and Snail mRNA but a significant downregulation of nephrin mRNA expression in T2D rats and T2D rats exposed to DEP while MH at 30 mg/kg was able to reverse these effects.

Kidney injury molecule 1 (KIM1), a type-1 transmembrane protein, is an emerging biomarker whose expression and release are induced in renal tubular cells after injury. It is a distinct immunoglobulin domain-containing epithelial cell adhesion molecule. The KIM1 mRNA and protein levels are modest in normal kidneys but considerably higher in post-ischemic kidneys (Song et al., 2019; Bonventre and Yang, 2011). There was up-regulation of KIM1 mRNA expression in T2D, DEP and T2D-DEP group, and it signifies increased renal injury. This effect was, however, ameliorated following treatment with MH.

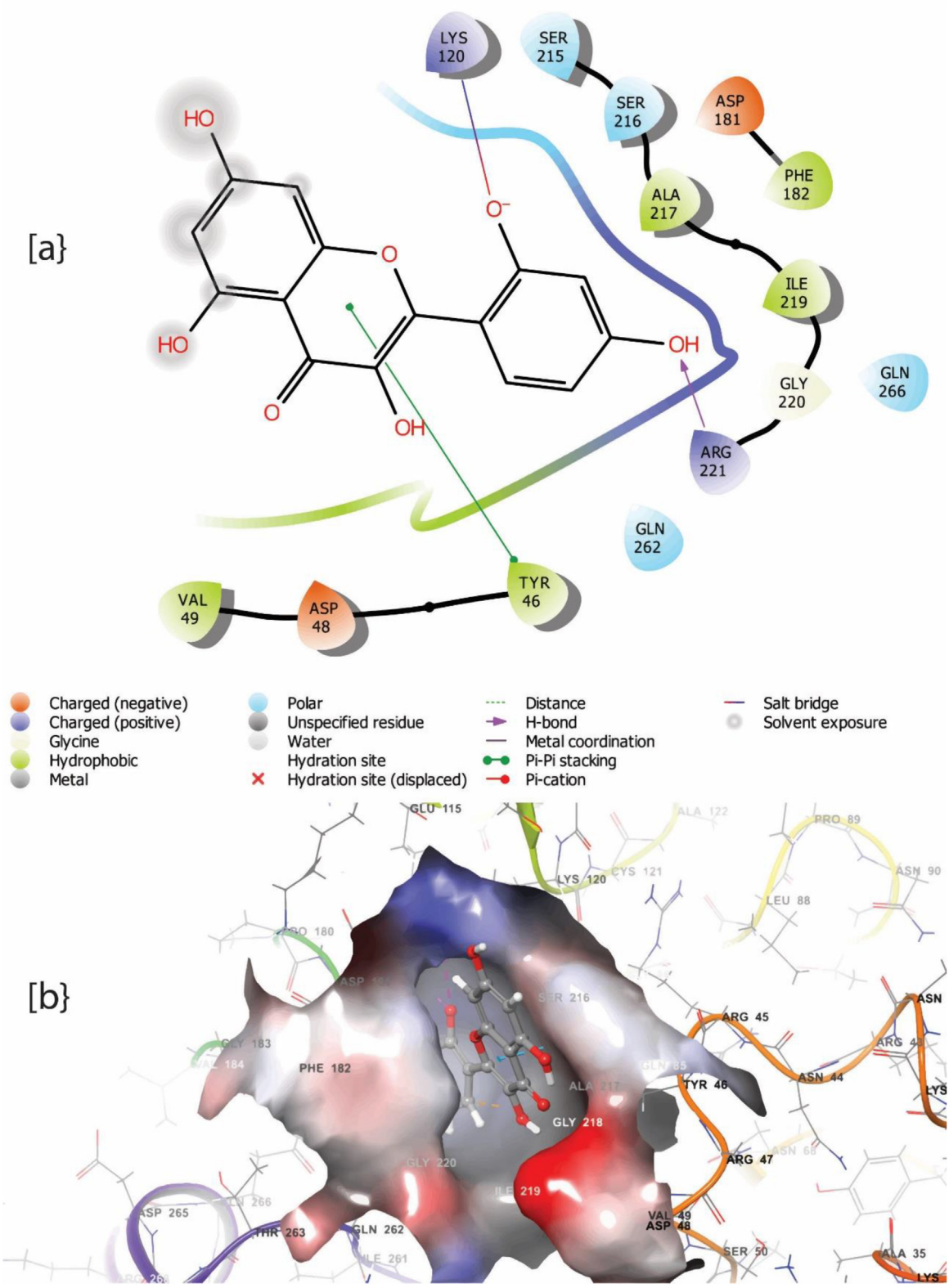

Fig. 8. Two- and three-dimensional interaction diagram between MH and notch1.

Molecular docking calculates the binding affinity of the small molecules within the binding pocket of a receptor (Olawale et al., 2022b). Docking results shows that MH had favorable binding affinity with angiotensin II, Notch1 and nephrin. The bioactive compound formed different non-covalent interactions such as H-bond, pi-pi stacking with the three proteins. Furthermore, MH formed a stable complex with these proteins' crystal structure. It is evidence that the molecular docking results supported the results obtained from the wet experiment.

5. Conclusion

This study has shown that DEP significantly increase the mRNA

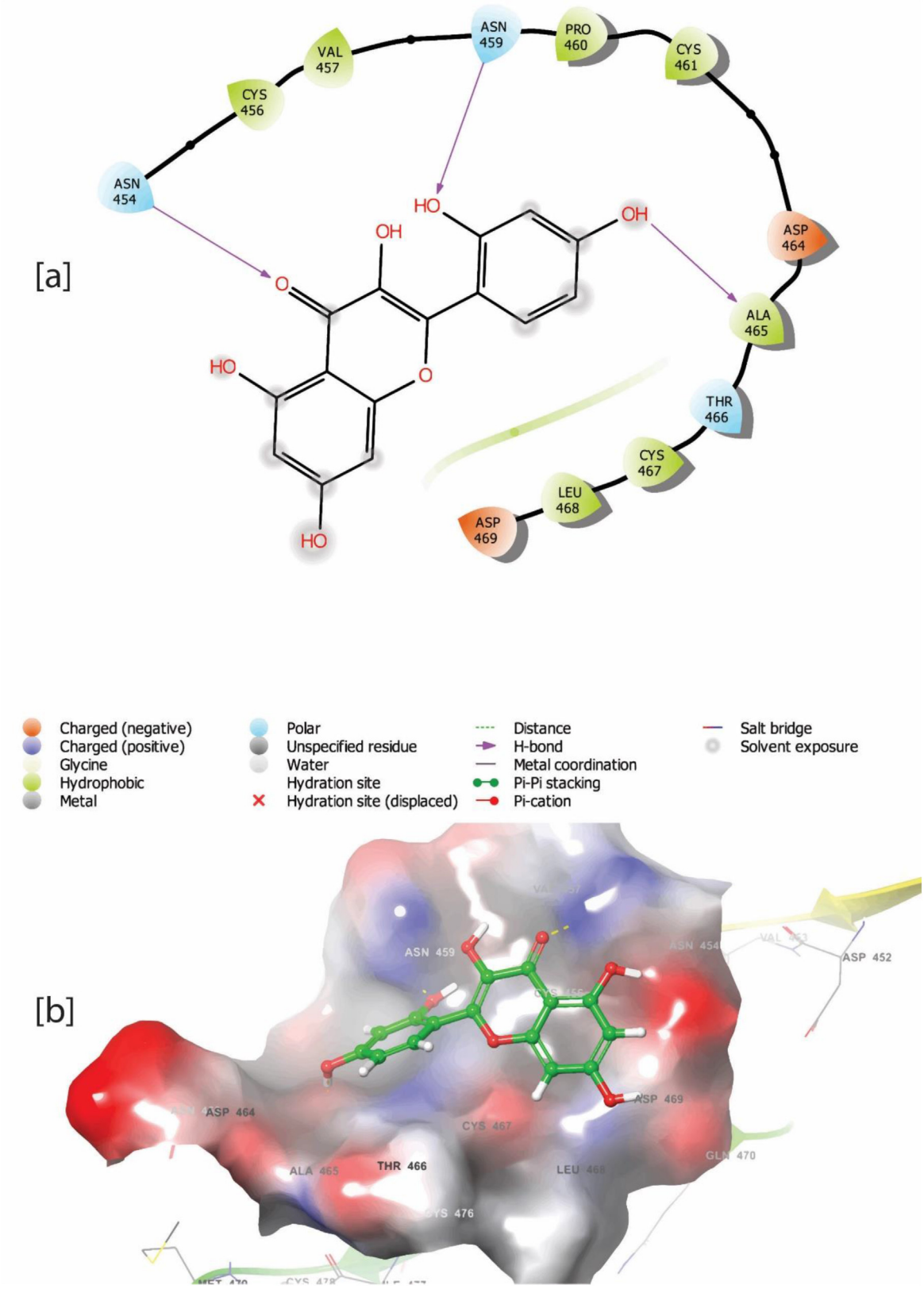

Fig. 9. [A] and [B] frontier molecular orbital, [C] molecular electrostatic potential; [D] fukui positive and [E] fukui negative of MH when dissolved in DMSO.

expression of KIM1, angiotensin II, notch1 and snail and significantly increase the mRNA expression of nephrin in T2D wistar rats. These effects were however ameliorated following treatment with MH. MH lowered the serum level of creatinine, urea and total protein; it also caused a significant reduction in the level of renal electrolytes. Finally, it also increased the mRNA expression of nephrin by modulating some

Table 4
Docking and post-docking analysis of morin hydrate and metformin with notch 1.

Compound name	Molecular docking studies				Binding free energy			
	Docking score	Interacting residues	No of H-bond	No of pi-pi interaction	ΔG_{Bind}[a]	ΔG_{Bind}[b] H-bond	ΔG_{Bind}[c] Coulomb	ΔG_{Bind}[d] vdW
Morin hydrate	−6.801	Asn454, Asn459, Ala465	3	–	−35.69	−2.58	−28.76	−26.05

[a] MM-GBSA free energy (kcal/mol) of binding.
[b] Contribution to the MM-GBSA free energy of binding (kcal/mol) from hydrogen bond.
[c] Contribution to the MMGBSA free energy of binding (kcal/mol) from the van der Waals energy.
[d] Contribution to the MM-GBSA free energy of binding (kcal/mol) from the Coulomb energy.

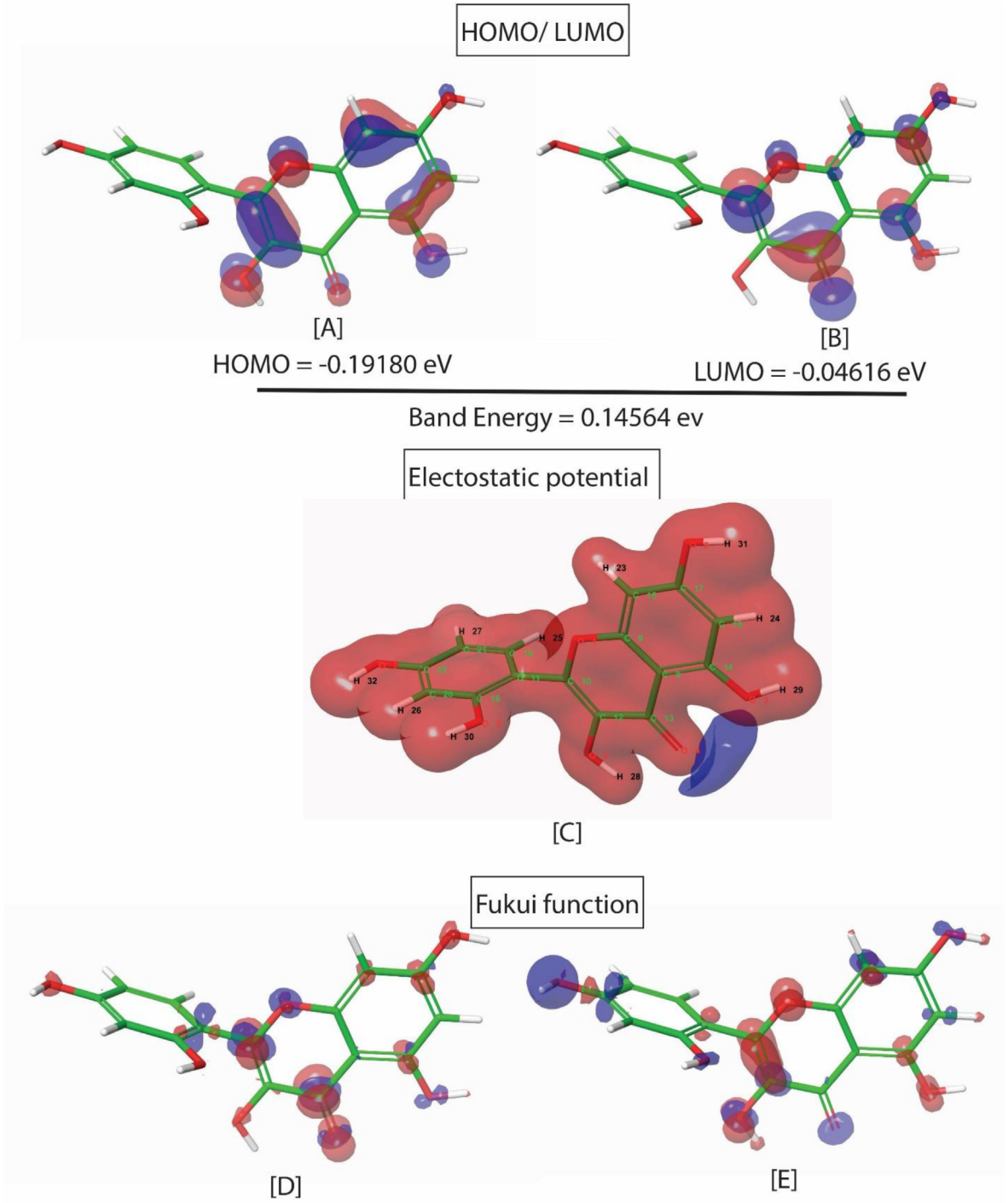

Fig. 10. [A] and [B] frontier molecular orbital, [C] molecular electrostatic potential; [D] fukui positive and [E] fukui negative of morin hydrate when dissolved in DMSO.

molecules in Notch1/Snail signalling pathway. Thus, this study suggests that MH preserves glomerular filtration and protects the kidney in T2D rats exposed to DEP.

Funding

This research work received no funding.

CRediT authorship contribution statement

All authors have accepted responsibility for the entire content of this manuscript and approved its submission. A.O.L: conceptualization, project design and supervision; I.M.F: data analysis, methodology, original drafting of the manuscript; O. A: data analysis, methodology, original drafting of the manuscript; O·F·K: manuscript editing; O·I: methodology and original drafting of the manuscript.

Ethical declaration

The experiments were performed in accordance with the National Guidelines for Experimental Animal Welfare and with approval of the Animal Welfare and Research Ethics Committee at Federal university of Technology, Akure, Nigeria (Ethical approval No: FUTA/ETH/2020/013).

Research funding

None declared.

Declaration of competing interest

The authors declare that they have no known competing financial interests or personal relationships that could have appeared to influence the work reported in this paper.

Acknowledgments

Not applicable.

Appendix A. Supplementary data

Supplementary data to this article can be found online at https://doi.org/10.1016/j.amolm.2023.100019.

References

Adachi, S., Sasaki, K., Kondo, S., Komatsu, W., Yoshizawa, F., Isoda, H., et al., 2020. Antihyperuricemic effect of urolithin A in cultured hepatocytes and model mice. Molecules 25, 5136.

Afkarian, M., Zelnick, L.R., Hall, Y.N., Heagerty, P.J., Tuttle, K., Weiss, N.S., et al., 2016. Clinical manifestations of kidney disease among US adults with diabetes, 1988-2014. JAMA 316, 602–610.

Albano, G.D., Montalbano, A.M., Gagliardo, R., Anzalone, G., Profita, M., 2022. Impact of air pollution in airway diseases: role of the epithelial cells (cell models and biomarkers). Int. J. Mol. Sci. 23, 2799.

Aleisa, A.M., Al-Rejaie, S.S., Abuohashish, H.M., Ahmed, M.M., Parmar, M.Y., 2013. Nephro-protective role of morin against experimentally induced diabetic nephropathy. Dig. J. Nanomater. Biostruct. 8, 395–401.

Bonventre, J v, Yang, L., 2011. Cellular pathophysiology of ischemic acute kidney injury. J. Clin. Invest. 121, 4210–4221.

Bowe, B., Xie, Y., Li, T., Yan, Y., Xian, H., Al-Aly, Z., 2018. The 2016 global and national burden of diabetes mellitus attributable to PM 2· 5 air pollution. Lancet Planet. Health 2, e301–e312.

Chen, L.-C., Lin, H.-Y., Lee, M.-S., Chiou, W.-Y., Huang, L.-W., Chew, C.-H., et al., 2021. Effectiveness of individual audio-visual coaching, respiratory modulated stereotactic body radiotherapy for localized hepatocellular carcinoma: analysis of 29 cases from a single academic radiotherapy center. Tzu Chi Med. J. 33, 380.

Chilian-Herrera, O.L., Tamayo-Ortiz, M., Texcalac-Sangrador, J.L., Rothenberg, S.J., López-Ridaura, R., Romero-Martínez, M., et al., 2021. PM2. 5 exposure as a risk factor for type 2 diabetes mellitus in the Mexico City metropolitan area. BMC Publ. Health 21, 1–10.

Ciobanu, A.O., Gherghinescu, C.L., Dulgheru, R., Magda, S., Galrinho, R.D., Florescu, M., et al., 2013. The impact of blood pressure variability on subclinical ventricular, renal and vascular dysfunction, in patients with hypertension and diabetes. Maedica (Bucur) 8, 129.

Costello, S., Attfield, M.D., Lubin, J.H., Neophytou, A.M., Blair, A., Brown, D.M., et al., 2018. Ischemic heart disease mortality and diesel exhaust and respirable dust exposure in the diesel exhaust in miners study. Am. J. Epidemiol. 187, 2623–2632.

Dal Canto, E., Ceriello, A., Rydén, L., Ferrini, M., Hansen, T.B., Schnell, O., et al., 2019. Diabetes as a cardiovascular risk factor: an overview of global trends of macro and micro vascular complications. Eur J Prev Cardiol 26, 25–32.

Elekofehinti, O.O., Iwaloye, O., Olawale, F., Chukwuemeka, P.O., Folorunso, I.M., 2021. Newly designed compounds from scaffolds of known actives as inhibitors of survivin: computational analysis from the perspective of fragment-based drug design. Silico Pharmacol 9, 1–16.

Gagliardini, E., Perico, N., Rizzo, P., Buelli, S., Longaretti, L., Perico, L., et al., 2013a. Angiotensin II contributes to diabetic renal dysfunction in rodents and humans via Notch1/Snail pathway. Am. J. Pathol. 183, 119–130.

Gagliardini, E., Perico, N., Rizzo, P., Buelli, S., Longaretti, L., Perico, L., et al., 2013b. Angiotensin II contributes to diabetic renal dysfunction in rodents and humans via Notch1/Snail pathway. Am. J. Pathol. 183, 119–130.

Gaw, A., Packard, C.J., Lindsay, G.M., Griffin, B.A., Caslake, M.J., Lorimer, A.R., et al., 1995. Overproduction of small very low density lipoproteins (Sf 20-60) in moderate hypercholesterolemia: relationships between apolipoprotein B kinetics and plasma lipoproteins. J. Lipid Res. 36, 158–171.

Gheith, O., Farouk, N., Nampoory, N., Halim, M.A., Al-Otaibi, T., 2016. Diabetic kidney disease: world wide difference of prevalence and risk factors. J Nephropharmacol 5, 49.

Griffin, B.R., Faubel, S., Edelstein, C.L., 2019. Biomarkers of drug-induced kidney toxicity. Ther. Drug Monit. 41, 213.

Jeong, H.-S., Ryoo, I., Kwak, M.-K., 2015. Regulation of the expression of renal drug transporters in KEAP1-knockdown human tubular cells. Toxicol. Vitro 29, 884–892.

Kapoor, R., Kakkar, P., 2012. Protective Role of Morin, a Flavonoid, against High Glucose Induced Oxidative Stress Mediated Apoptosis in Primary Rat Hepatocytes.

Kittell, F., 2012. Diabetes management. Nutrit. Ther. Chronic Kidney Disease 197–212.

Klemens, C.A., Brands, M.W., Staruschenko, A., 2019. Postprandial effects on electrolyte homeostasis in the kidney. Am. J. Physiol. Ren. Physiol. 317, F1405–F1408.

Landrigan, P.J., Fuller, R., Acosta, N.J.R., Adeyi, O., Arnold, R., Baldé, A.B., et al., 2018. The Lancet Commission on pollution and health. Lancet 391, 462–512.

Lawal, A.O., Zhang, M., Dittmar, M., Lulla, A., Araujo, J.A., 2015. Heme oxygenase-1 protects endothelial cells from the toxicity of air pollutant chemicals. Toxicol. Appl. Pharmacol. 284, 281–291.

Lawal, A.O., Folorunso, I.M., Iwaloye, O., 2022. MH protects type-2-diabetic wistar rats exposed to diesel exhaust particles from inflammation and oxidative stress. J. Diabetes Metab. Disord. 1–12.

Li, C., Siragy, H.M., 2014. High glucose induces podocyte injury via enhanced (pro) renin receptor-Wnt-β-catenin-snail signaling pathway. PLoS One 9, e89233.

Liu, F., Ma, G., Tong, C., Zhang, S., Yang, X., Xu, C., et al., 2022. Elevated blood urea nitrogen-to-creatinine ratio increased the risk of Coronary Artery Disease in patients living with type 2 diabetes mellitus. BMC Endocr. Disord. 22, 1–10.

Ma, R., Liu, L., Liu, X., Wang, Y., Jiang, W., Xu, L., 2013. Triptolide markedly attenuates albuminuria and podocyte injury in an animal model of diabetic nephropathy. Exp. Ther. Med. 6, 649–656.

Maremonti, F., Meyer, C., Linkermann, A., 2022. Mechanisms and models of kidney tubular necrosis and nephron loss. J. Am. Soc. Nephrol. 33, 472–486.

Moosaie, F., Abhari, S.M.F., Deravi, N., Behnagh, A.K., Esteghamati, S., Firouzabadi, F.D., et al., 2021. Waist-to-height ratio is a more accurate tool for predicting hypertension than waist-to-hip circumference and BMI in patients with type 2 diabetes: a prospective study. Front. Public Health 9.

Mora-Fernández, C., Domínguez-Pimentel, V., de Fuentes, M.M., Górriz, J.L., Martínez-Castelao, A., Navarro-González, J.F., 2014. Diabetic kidney disease: from physiology to therapeutics. J. Physiol. 592, 3997–4012.

Olawale, F., Iwaloye, O., Folorunso, I.M., Shityakov, S., 2022a. In silico high throughput screening of ZINC database of natural compounds to identify novel histone deacetylase inhibitors. J. Comput. Biophys. Chem. 22, 11–30.

Olawale, F., Olofinsan, K., Iwaloye, O., Chukwuemeka, P.O., Elekofehinti, O.O., 2022b. Screening of compounds from Nigerian antidiabetic plants as protein tyrosine phosphatase 1B inhibitor. Computational Toxicology 21. https://doi.org/10.1016/j.comtox.2021.100200.

Pálsson, R., Patel, U.D., 2014. Cardiovascular complications of diabetic kidney disease. Adv. Chron. Kidney Dis. 21, 273–280.

Paoli, P., Cirri, P., Caselli, A., Ranaldi, F., Bruschi, G., Santi, A., et al., 2013. The insulin-mimetic effect of Morin: a promising molecule in diabetes treatment. Biochim. Biophys. Acta Gen. Subj. 1830, 3102–3111.

Pasquel, F.J., Umpierrez, G.E., 2014. Hyperosmolar hyperglycemic state: a historic review of the clinical presentation, diagnosis, and treatment. Diabetes Care 37, 3124–3131.

Raines, R., McKnight, I., White, H., Legg, K., Lee, C., Li, W., et al., 2022. Drug-targeted genomes: mutability of ion channels and GPCRs. Biomedicines 10, 594.

Rajput, S.A., Wang, X., Yan, H.-C.M.H., 2021. A comprehensive review on novel natural dietary bioactive compound with versatile biological and pharmacological potential. Biomed. Pharmacother. 138, 111511.

Ramsey, D.W., Bright, S.W., Ludlow, J.W., Winston, V., 1986. Detection of infectious pancreatic necrosis virus using an inhibition enzyme-linked immunosorbent assay. J. Immunoassay 7, 229–239.

Salazar, J.H., 2014. Overview of urea and creatinine. Lab. Med. 45, e19–e20.

Shi, G., Wu, W., Wan, Y.-G., Hex, H.W., Tu, Y., Han, W.-B., et al., 2018. Low dose of triptolide ameliorates podocyte epithelial-mesenchymal transition induced by high

dose of D-glucose via inhibiting Wnt3α/β-catenin signaling pathway activation. Zhongguo Zhongyao Zazhi 43, 139–146.
Singh, M.P., Chauhan, A.K., Kang, S.C., 2018. MH ameliorates cisplatin-induced ER stress, inflammation and autophagy in HEK-293 cells and mice kidney via PARP-1 regulation. Int. Immunopharm. 56, 156–167.
Song, J., Yu, J., Prayogo, G.W., Cao, W., Wu, Y., Jia, Z., et al., 2019. Understanding kidney injury molecule 1: a novel immune factor in kidney pathophysiology. Am J Transl Res 11, 1219.
Sylla, F.K., Faye, A., Fall, M., Anta, T.-D., 2017. Air pollution related to traffic and chronic respiratory diseases (asthma and COPD) in Africa. Health N Hav 9, 1378–1389.
Tong, H., Rappold, A.G., Diaz-Sanchez, D., Steck, S.E., Berntsen, J., Cascio, W.E., et al., 2012. Omega-3 fatty acid supplementation appears to attenuate particulate air pollution–induced cardiac effects and lipid changes in healthy middle-aged adults. Environ. Health Perspect. 120, 952–957.
Tonneijck, L., Muskiet, M.H.A., Smits, M.M., van Bommel, E.J., Heerspink, H.J.L., van Raalte, D.H., et al., 2017. Glomerular hyperfiltration in diabetes: mechanisms, clinical significance, and treatment. J. Am. Soc. Nephrol. 28, 1023–1039.
Tuttle, K.R., 2017. Back to the future: glomerular hyperfiltration and the diabetic kidney. Diabetes 66, 14–16.
Vallon, V., Komers, R., 2011. Pathophysiology of the diabetic kidney. Compr. Physiol. 1, 1175.
Warren, A.M., Knudsen, S.T., Cooper, M.E., 2019. Diabetic nephropathy: an insight into molecular mechanisms and emerging therapies. Expert Opin. Ther. Targets 23, 579–591.
Welsh, G.I., Saleem, M.A., 2012. The podocyte cytoskeleton—key to a functioning glomerulus in health and disease. Nat. Rev. Nephrol. 8, 14–21.
Yao, M., Wang, X., Wang, X., Zhang, T., Chi, Y., Gao, F., 2015. The Notch pathway mediates the angiotensin II-induced synthesis of extracellular matrix components in podocytes. Int. J. Mol. Med. 36, 294–300.
Yaser, H.S., Narges, K., Yaser, S., Rasoul, M., 2014. Air pollution and cardiovascular mortality in Kerman from 2006 to 2011. American J. Cardiovasc. Disease Res. 2, 27–30.
Yokota, T., Shibata, N., Ura, T., Takahari, D., Shitara, K., Muro, K., et al., 2010. Cycleave polymerase chain reaction method is practically applicable for V-Ki-ras2 Kirsten rat sarcoma viral oncogene homolog (KRAS)/V-raf murine sarcoma viral oncogene homolog B1 (BRAF) genotyping in colorectal cancer. Transl. Res. 156, 98–105.
Zhu, J., Zheng, X., 2021. Clinical value of INSL3 in the diagnosis and development of diabetic nephropathy. J. Clin. Lab. Anal. 35, e23898.